

Document downloaded from:

<http://hdl.handle.net/10251/176097>

This paper must be cited as:

Nadal, L.; Coupé, P.; Helmer, C.; Manjón Herrera, JV.; Amieva, H.; Tison, F.; Dartigues, J.... (2020). Differential annualized rates of hippocampal subfields atrophy in aging and future Alzheimer's clinical syndrome. *Neurobiology of Aging*. 90:75-83.
<https://doi.org/10.1016/j.neurobiolaging.2020.01.011>



The final publication is available at

<https://doi.org/10.1016/j.neurobiolaging.2020.01.011>

Copyright Elsevier

Additional Information

Differential annualized rates of hippocampal subfields atrophy in aging and future Alzheimer's clinical syndrome

Louis Nadal^{1,2}; Pierrick Coupé³; Catherine Helmer⁴; José V. Manjon⁵; Helene Amieva⁴; François Tison^{1,2}; Jean-François Dartigues^{2,4}; Gwénaëlle Catheline^{6,7} and Vincent Planche^{1,2}

1. Univ. Bordeaux, CNRS, Institut des Maladies Neurodégénératives, UMR 5293, F-33000 Bordeaux, France
2. Centre Mémoire de Ressources et de Recherches, Pôle de Neurosciences Cliniques, CHU de Bordeaux, F-33000 Bordeaux, France
3. Univ. Bordeaux, CNRS, Laboratoire Bordelais de Recherche en Informatique, UMR 5800, PICTURA, F-33405 Talence, France
4. Univ. Bordeaux, Inserm, Bordeaux Population Health Research Center, UMR 1219, F-33000 Bordeaux, France
5. Instituto de Aplicaciones de las Tecnologías de la Información y de las Comunicaciones Avanzadas (ITACA), Universitat Politècnica de València, 46022 Valencia, Spain.
6. EPHE, PSL, F-33000 Bordeaux, France
7. Univ. Bordeaux, CNRS, Institut de Neurosciences cognitives et intégratives d'Aquitaine, UMR 5287, F-33000 Bordeaux, France

Corresponding author: Dr Vincent Planche, MD., PhD., Institut des Maladies Neurodégénératives, UMR CNRS 5293, Centre Broca Nouvelle-Aquitaine, 146 rue Léo Saignat – 33076 Bordeaux cedex, France; vincent.planche@u-bordeaux.fr; Phone: +33 533 51 47 19

Word count: abstract: 200; article: 3861

Tables/Figures: 3 tables, 3 figures

References: 54

Abstract

Several studies have investigated the differential vulnerability of hippocampal subfields during aging and Alzheimer's disease (AD). Results were often contradictory, mainly because these works were based on concatenations of cross-sectional measures in cohorts with different ages or stages of AD, in the absence of a longitudinal design. Here, we investigated 327 participants from a population-based cohort of non-demented older adults with a 14-year clinical follow-up. MRI at baseline and 4 years later were assessed to measure the annualized rates of hippocampal subfields atrophy in each participant using an automatic segmentation pipeline with subsequent quality-control. In the one hand, CA4-dentate gyrus was significantly more affected than the other subfields in the whole population (CA1-3: -0.68%/year; subiculum: -0.99%/year and CA4-DG: -1.39%/year; $p < 0.0001$). In the other hand, the annualized rate of CA1-3 atrophy was associated with an increased risk of developing Alzheimer's clinical syndrome over time, independently of age, gender, educational level and ApoE4 genotype (HR=2.0; IC95% 1.4-3.0). These results illustrate the natural history of hippocampal subfields atrophy during aging and AD by showing that the dentate gyrus is the most vulnerable subfield to the effects of aging while the cornu-ammonis is the primary target of AD pathophysiological processes, years prior to symptom onset.

Key words: MRI; Hippocampal subfields; aging; Alzheimer's disease

Introduction

The hippocampus is an archeocortical structure involved in cognitive functions such as memory and spatial learning. The hippocampal formation is made up of distinct subfields that include the subiculum, the cornu-ammonis (CA1-4) and the dentate gyrus. Although the hippocampus is non-specifically affected by almost all neurological and psychiatric disorders, its subfields can be differentially and selectively affected by different pathologies, including Alzheimer's disease (AD) (Small et al., 2011), neurovascular damage (Li et al., 2016), temporal lobe epilepsy (Sone et al., 2016), multiple sclerosis (Planche et al., 2018), mood disorders (Cao et al., 2017), schizophrenia (Ho et al., 2017) or post-traumatic stress disorder (Postel et al., 2019). Theoretically, the study of hippocampal focal vulnerability could explain this phenotypic diversity and might distinguish between various normal and pathological conditions.

Hippocampal damage in patients with AD was first histologically described using post-mortem brains (Ball et al., 1985) and was subsequently demonstrated *in vivo* using MRI. Such studies revealed strong correlations between MRI and histological data regarding hippocampal volume and neuronal counts (Bobinski et al., 2000). Therefore, hippocampal atrophy can be used as a biomarker of neuronal injury in AD and as information in support of diagnostic criteria (Scheltens et al., 1992; McKhann et al., 2011). However, as mentioned above, hippocampal atrophy is poorly specific of AD and is often present in patients with other causes of dementia such as frontotemporal lobar degeneration, vascular dementia and hippocampal sclerosis, as well as in healthy aging (Harper et al., 2014; Coupé et al., 2017).

The first pathological studies to identify focal hippocampal damage in AD reported severe neuronal loss in the CA1 region (West et al., 1994). Consistent with these findings, the majority of neuroimaging studies investigating patients with AD have reported that regional atrophy is primarily located in CA1 (De Flores et al., 2015). These findings seem consensual between studies using surface-based techniques (Csernansky et al., 2000; Chételat et al., 2008; Frisoni et al., 2008; Tang et al., 2014) but are more in contradiction with studies using proper volumetric analyses, in which diffuse atrophy of the hippocampus was observed (although usually more severe in CA1) (Mueller et al., 2010; Kerchner et al., 2013; La Joie et al., 2013). The idea of selective regional vulnerability in the hippocampus during healthy aging is even more controversial (see de Flores et al., 2015 for review). Interestingly, a recent MRI-histological correlation study demonstrated that the modification of hippocampal subfields shape during aging is associated with AD-related tau pathology, but not with amyloid beta or TDP-43 pathologies (Hanko et al., 2019). It suggests that the monitoring of hippocampal subfields damage in elderly people could help clinicians distinguish between healthy aging, the early stages of AD, and other causes of neurodegenerative dementia. Furthermore, as a biomarker of confined tauopathy, it is possible that the early detection of hippocampal subfields atrophy during aging could help to predict future AD.

The discrepancies between the MRI studies assessing hippocampal subfields integrity in aging and AD can be explained in several ways. First, many of them included small samples, with significant heterogeneity in terms of the subject's sociodemographic and clinical characteristics. Second, these studies relied on cross-sectional MRI acquisition procedures that cannot properly measure individual occurrences of atrophy, which is a dynamic process measured between two timepoints. Third, none of these studies conducted long-term longitudinal follow-ups of participants that would have allowed for the determination of individual cognitive trajectories to differentiate healthy aging from various neurodegenerative diseases properly. Fourth, most of these MRI studies employed surface-based mesh modelling techniques to study the shape of the hippocampus. However, measuring external surface modifications does not allow for a direct characterization of the inner alterations of a particular subfield (particularly the dentate gyrus), which would require volumetric measures (De Flores et al., 2015).

Thus, the primary aim of the present study was to assess properly the natural history of hippocampal subfields vulnerability during healthy aging and in elderly people who will develop Alzheimer's clinical syndrome over time. Additionally, we aimed at investigating whether the annualized rates of hippocampal subfields atrophy could predict an increased risk of Alzheimer's clinical syndrome over time. For these purposes, a well-defined population-based cohort of older adults who underwent two MRI examinations at a 4-year interval and also completed a clinical follow-up period for up to 14 years was evaluated. This long-term clinical follow-up allowed to truly discriminate subjects developing AD pathology from subjects remaining free of dementia over time.

Methods

Participants

The study participants were recruited from the Bordeaux subset of the Three-City (3C) study, which was a longitudinal population-based cohort designed to evaluate the risk factors of dementia (3C Study Group, 2003). During the 1999-2000 inclusion period, non-institutionalized individuals who were 65 years of age and older were randomly selected from electoral lists and then followed-up prospectively for up to 14 years. Information regarding demographic characteristics and ApoE genotype was collected at baseline. Methods for genotyping the ApoE epsilon polymorphism have been described previously (Dufouil et al., 2005) and ApoE4 carrier was defined as the presence of at least one E4 allele. Of the initial cohort of participants with baseline MRI data (n=663), only non-demented participants with a MMSE>23, who agreed to have a second MRI 4 years later were included in the present hippocampal subfields analyses (n=364) (Fig. 1A and B). There were no significant differences in the baseline

demographic or neuropsychological characteristics between subjects who completed one MRI and those who completed two MRIs. All participants provided written informed consent to participate and the study protocol was approved by the ethics committee of Kremlin-Bicêtre University Hospital (Paris, France).

Neuropsychological assessments and diagnosis of Alzheimer's clinical syndrome

During the 14-year follow-up period, neuropsychological assessments were administered by trained psychologists at baseline and after 2, 4, 7, 10, 12 and 14 years (Fig. 1A). At each follow-up visit, a diagnosis of dementia was pre-specified at home by the neuropsychologist and a clinical validation of the diagnosis was made at home by a neurologist or a geriatrician. A definitive diagnosis of dementia and diagnoses of possible or probable AD were ultimately made by a panel of independent neurologists based on the Diagnostic and Statistical Manual of Mental Disorders criteria (DSM-IV) and the National Institute of Neurological and Communicative Diseases and Stroke/Alzheimer's Disease and Related Disorders Association criteria (McKhann et al., 2011). Cases of probable or possible AD were labeled as "Alzheimer's clinical syndrome" according to the recent National Institute on Aging and Alzheimer's Association (NIA-AA) research framework recommendations (Jack et al., 2018). According to these definitions, people with mild cognitive impairment at the end of the follow-up were not considered as demented and were therefore classified in the "non-AD group".

The initial neuropsychological battery consisted of the Mini Mental State Evaluation (MMSE: global cognitive functions), the Free and Cued Selective Reminding Test (FCSRT: verbal episodic memory - sum of the number of words retrieved during the three free or cued trials), the Benton Visual Retention Test (BVRT: visuospatial working memory), the Isaacs Set Test (IST: semantic fluency) and the Trail Making Test part A and B (TMT-A and TMT-B: attention, information processing speed and executive functions ((number of correct moves/total time)x10)).

MRI acquisition and processing

Participants were scanned on a 1.5 T Gyroscan Intera system (Philips Medical Systems) with a quadrature head coil. The morphological protocol consisted of 3D high-resolution T1-weighted images acquired in transverse plane using magnetization prepared rapid gradient echo sequence (TR=8.5 ms, TE=3.9 ms, $\alpha=10^\circ$, FOV=240 mm, voxel size=0.94x0.94x1mm³). The same scanner and the same sequence were used for the baseline and the 4-year follow-up MRI procedures.

For the volumetric analyses of brain structures (total hippocampal volume, total grey matter volume and total intracranial volume) and hippocampal subfields, T1-weighted images were processed using the volBrain system (<http://volbrain.upv.es>) (Manjón and Coupé, 2016). After denoising with an adaptive nonlocal mean filter (Manjón et al., 2010), the images were affine-registered into the Montreal Neurological Institute (MNI) space using ANTS software (Avants et al., 2011), corrected for image inhomogeneities using N4 (Tustison et al., 2010) and then intensity-normalized (Nyúl and Udupa, 1999). Next, the segmentation of hippocampal subfields was performed with the HIPS pipeline (Romero et al., 2017), based on a combination of non-linear registration and multiatlas patch-based label fusion with systematic error correction. This method uses a training library from a public repository (www.nitrc.org/projects/mni-hisub25) composed of high resolution T1w images manually labeled (Kulaga-Yoskovitz et al., 2015). We used Kulaga-Yoskovitz protocol instead of Winterburn protocol because its segmentations were more reliable (0.88 vs 0.71) due to the use of a larger number of training cases (Romero et al., 2017). To perform the segmentation, the images were up-sampled with a local adaptive super resolution method to fit in the training image resolution (Fig. 2A). (Coupé et al., 2013). The method provides automatic segmentation of hippocampal subfields gathered into 3 labels, based on morphology and intensity of densely myelinated molecular layers as follows: Subiculum, CA1-3 and CA4/dentate gyrus (CA4-DG) (Fig. 2B).

Quality control of the image-processing pipeline for the baseline and 4-year MRI data was performed by two neurologists (LN and VP) who were blind to the final dementia diagnosis using 3D Slicer 4.10.0 (www.slicer.org). First, a visual assessment of the image processing quality for all subjects (n=364, at 2 timepoints) was performed using sagittal, coronal and axial slices of the 3D hippocampal volume. Registration into the MNI space, intracranial volume extraction and tissue classification were also carefully evaluated. This step led to the removal of 37 subjects from the study due to segmentation errors that were deemed too important to be corrected. Second, we performed manual correction of 44 labels with minor segmentation errors (such as the inappropriate inclusion of choroidal plexus, parahippocampal T1-hypointensity, and/or CSF “pockets”). Finally, the present cohort consisted of 327 participants with available quality-controlled hippocampal subfields segmentations at both baseline and 4 years (Fig. 2B). Using these longitudinal MRI data, the annualized rates of atrophy for each participant were calculated as follows: $((\text{volume after 4 years} - \text{volume at baseline})/\text{volume at baseline})/4$.

Statistical analyses

Statistical analyses were performed with Prism software 8 (Graphpad) and XLstats 19.4 (Addinsoft). First, participants who were seen at least one time after the second MRI for a new neuropsychological assessment were classified as “incident-AD” (n=35) and “non-AD” (n=269) based on the final diagnosis after the 14-year longitudinal follow-up period (Fig. 1B). We compared clinical and imaging

characteristics at baseline between groups using t-tests for quantitative variables and Chi-squared tests for categorical variables. Second, to describe differential hippocampal subfields atrophy during aging and AD, the annualized rates of atrophy in the three subfields were compared using one-way and two-way analysis of variance tests (ANOVA) for the whole cohort of participants and for the “incident-AD” and “non-AD” groups, respectively. ANOVAs were followed by appropriate *post-hoc* tests (Sidak’s or Holm-Sidak’s) to account for multiple comparisons. Cohen’s d was used to determine the effect size of atrophy rates between the “incident-AD” and “non-AD” groups. Third, associations between baseline characteristics and the annualized rates of hippocampal subfields atrophy were assessed using t-tests, Pearson correlation coefficients and multiple linear regressions (using Bonferroni correction for multiple comparisons when appropriate). Finally, to identify which hippocampal subfields might be predictive of incident Alzheimer’s clinical syndrome over time, Cox proportional hazard survival regression analyses were performed, using the annualized rates of atrophy as predictors and typical confounding variables, such as age, gender, education level and ApoE4 genotype as co-variates.

Results

Demographic, neuropsychological and MRI characteristics at baseline

Three-hundred and twenty-seven participants were finally included in our analyses after quality control and manual correction of the automatic hippocampal subfields segmentation procedures at both timepoints. Of these participants, 304 (92.7%) were seen at least one time after the second MRI for a new neuropsychological assessment (Fig 1B). During the 14-year longitudinal follow-up period, 35 participants developed Alzheimer’s clinical syndrome after the second MRI (12% of participants, “incident-AD”). The mean time before the estimated conversion to dementia was 11.5 years (± 2.2). The baseline characteristics of the whole sample and of the two subgroups are summarized in Table 1.

Participants who developed incident Alzheimer’s clinical syndrome were significantly older at baseline than the group of participants who remained free of AD over time (73.7 vs 71.7 years, $p=0.003$). In term of baseline neuropsychological characteristics, the “incident-AD” group already displayed poorer performance in tests of verbal episodic memory tests (free recall of the FCRST, $p=0.002$), visuospatial working memory (BVRT, $p=0.003$) and attentional and executive function (TMT-A and TMT-B, $p=0.001$ and $p=0.05$ respectively).

There were no significant differences in the baseline MRI characteristics between the “incident-AD” and “non-AD” groups.

Dynamics of regional hippocampal atrophy

The annualized rates of hippocampal subfields atrophy were calculated based on MRI collected at baseline and 4 years later. Analyses revealed a differential regional vulnerability in the hippocampus during aging (Fig. 3A). In the whole cohort, CA4-DG was significantly more affected than the other subfields whereas CA1-3 was significantly less affected (CA1-3: -0.68%/year; Subiculum: -0.99%/year and CA4-DG: -1.39%/year; $F=19.7$, $p<0.0001$ (ANOVA); mean differences: CA4-DG vs CA1-3 = -0.70, $p<0.0001$; Subiculum vs CA1-3 = -0.31, $p<0.01$ and CA4-DG vs Subiculum = -0.40, $p<0.01$ (Holm-Sidak's multiple comparisons test)). As a comparison, the annualized rate of atrophy was -0.84%/year in the whole hippocampus and -0.11%/year for the whole cerebral grey matter.

A two-way ANOVA accounting for incident Alzheimer's clinical syndrome revealed a "subfield effect" ($F=10.3$, $p<0.0001$) as well as a "disease effect" ($F=29.4$, $p<0.0001$) that could explain the variance in the annualized rates of regional hippocampal atrophy; without any significant interactions ($F=1.01$, $p=0.23$). Compared to the "non-AD" group, the "incident-AD" group had significantly higher rates of atrophy in CA1-3 (-1.37%/year vs -0.59%/year; $p<0.001$) and in CA4-DG (-2.33%/year vs -1.21%/year; $p<0.001$) but not in the subiculum. Regarding effect size, CA1-3 was the most affected subfield in the "incident-AD" group compared to the "non-AD" group ($d=0.77$ for CA1-3 and $d=0.50$ for CA4-DG) (Fig. 3B).

Associations between baseline characteristics and annualized rates of hippocampal subfields atrophy.

Age, gender, educational level and ApoE genotype were not associated or correlated with the annualized rate of hippocampal subfields atrophy in the whole cohort of participants and in the "non-AD" subgroup. Age, gender and educational level were not associated with the annualized rates of hippocampal subfields atrophy in the "incident-AD" group. However, there were associations between ApoE4 genotype and a higher annualized rates of atrophy in the subiculum ($p=0.028$) and CA1-3 ($p=0.030$) in the "incident-AD" subgroup (but these results were just below Bonferroni threshold p -values for multiple comparisons (0.016)). Associations between ApoE status and annualized rate of hippocampal subfields atrophy are summarized in Table 2.

Regarding the neuropsychological correlates at baseline, there was a significant association between the total recall score on the FCSRT and the annualized rate of atrophy in the CA1-3 ($r=0.18$, $p=0.0015$), taking into account multiple comparisons (Bonferroni threshold p -values = 0.0018 for 27 comparisons). This association was still significant after adjusting for age, educational level and ApoE4 status ($p=0.0016$).

Prediction of incident Alzheimer's clinical syndrome

The results of the Cox proportional hazard models assessing relationships of the annualized rates of hippocampal subfield atrophy, age, gender, educational level, and ApoE4 genotype with the risk of developing Alzheimer's clinical syndrome are shown in Table 3. In terms of regional hippocampal vulnerability, only the annualized rate of CA1-3 atrophy was associated with an increased risk of developing AD over time (HR=1.8; IC95% 1.2-2.6). This association remained significant after adjusting for age, gender, educational level and ApoE4 genotype (HR=2.0; IC95% 1.4-3.0).

In contrast, normalized hippocampal subfields volumes at baseline were not predictive of incident Alzheimer's clinical syndrome over time.

Discussion

Thanks to its longitudinal design involving repeated MRI exams and a 14-year clinical follow-up of 327 initially non-demented elderly people, this study showed that hippocampal subfields are differentially affected in healthy aging and AD. Indeed, we have shown that the annualized rate of CA4/dentate gyrus atrophy was the most important during aging, compared to the other hippocampal subfields. Additionally, we showed that participants who developed incident Alzheimer's clinical syndrome during the follow-up period had higher atrophy rates in CA4/dentate gyrus and CA1-3 compared to those who did not develop AD, but with a larger effect size in CA1-3. Our assumption is that the "neurodegenerative effect" linked to ongoing early AD pathophysiological process mainly affects CA1-3, on top of the aging-related atrophy in the dentate gyrus. Furthermore, participants with a higher initial annualized rate of CA1-3 atrophy had a higher risk of developing Alzheimer's clinical syndrome during the 14-year follow-up period, independently of age, gender, educational level, and ApoE4 genotype, whereas subicular and CA4/dentate gyrus atrophy were not predictive. The fact that the the annualized rate of CA1-3 was associated with lower FCSRT scores at baseline, known to predict dementia in this cohort (Auriacombe et al., 2010) and able to screen for patients with amnesic syndrome of the hippocampal in prodromal AD support this finding (Sarazin et al., 2007). Furthermore, ApoE4 genotype was associated with the annualized rate of CA1-3 atrophy only in the "incident-AD" group, which further strengthens the association of CA1-3 atrophy and AD pathophysiology. Taken together, these results revealed a differential vulnerability of CA4/dentate gyrus to aging process and a differential and early vulnerability of CA1-3 to AD pathology, even several years prior to the onset of dementia.

Many previous MRI studies have demonstrated that the hippocampus shrinks with age and that this shrinkage is not homogeneous among the hippocampal subfields. However, these previous studies were based on cross-sectional analyses that assessed hippocampal volume in subjects of different ages rather than the rate of atrophy over time in individual subjects (de Flores et al., 2015). Furthermore, these studies often failed to isolate participants free of age-related neurological diseases affecting the hippocampal circuit, because they lacked very long-term longitudinal follow-up periods. It may explain the significant discrepancies among the results. For example, some authors concluded that predominant damage during aging occurs either within CA1 (Kerchner et al., 2013; Raz et al., 2015; Daugherty et al., 2016), whereas others identified the subiculum (La Joie et al., 2010), the dentate gyrus (Pereira et al., 2014; Dillon et al., 2017), and still others observed homogeneous damage among various subfields (Mueller and Weiner, 2009; Apostolova et al., 2012; Malykhin et al., 2017). By conducting 4-year longitudinal MRI analyses in people over 65 (mean age 72), our work is therefore unique in demonstrating that individuals recruited from the general population who remained free of Alzheimer's clinical syndrome 10 years after the last MRI, exhibited a maximal annualized rate of atrophy in CA4/dentate gyrus (-1.21%/year) that was more than twice as high as in CA1-3. This CA4/dentate gyrus atrophy over time was even higher in participants who developed Alzheimer's clinical syndrome during the follow-up period (-2.33%/year). The dentate gyrus is the only neurogenic niche within the hippocampus and the differential atrophy observed in the present study is therefore well supported by animal and human studies investigating decreases in adult neurogenesis in the subgranular zone of the dentate gyrus during aging, that is further impaired during AD (Sorrells et al., 2018).

Our longitudinal findings showing an early vulnerability of CA1-3 during the AD pathophysiological process are consistent with most of the past and current histological and imaging cross-sectional studies (West et al., 1994; Kerchner et al., 2010; Fouquet et al., 2012; La Joie et al., 2013). The association between ApoE4 genotype and the rate of CA1-3 atrophy observed in the present study also corroborates data from a previous cross-sectional study that used a 7T-MRI scanner (Kerchner et al., 2014). Furthermore, we also found that the annualized rate of CA1-3 atrophy was associated with baseline FCSRT scores, assessing episodic memory, which is consistent with a previous cross-sectional voxel-based morphometry study showing that CA1 atrophy in patients with AD is associated with the severity of amnesic syndrome of the hippocampal type, which is the typical neuropsychological presentation of AD (Sarazin et al., 2010). Thus, our results extend previous knowledge by demonstrating that specific CA1-3 atrophy was associated with a higher risk of developing Alzheimer's clinical syndrome over a long period of time, independently of age, gender, educational level and ApoE4 genotype, even if this region was not the most atrophied subfield. From a pathophysiological point of view, these results support the hypothesis that tau neurofibrillary tangles initially spread from the entorhinal cortex to the cornu-ammonis of the hippocampus several years prior to symptom onset and that this process can be monitored *in vivo* with MRI (Braak and Braak, 1991; Lace et al., 2009).

The present results indicate that the longitudinal monitoring of hippocampal subfield atrophy may distinguish hippocampal damage linked to aging from that associated with AD. Interestingly, a previous study by our research group using the same cohort of older adults found that the atrophy rate of the whole hippocampus was not significantly associated with the incidence of Alzheimer’s clinical syndrome over time, which suggests that the rate of atrophy in specific hippocampal subfields is more informative than the rate of atrophy for the whole hippocampus (Planche et al., 2019). That study also revealed that individuals with “hippocampal predominant atrophy” (based on the evolution of hippocampal-to-cortical volume ratio over time) have a higher risk of developing Alzheimer’s clinical syndrome during a 12-year follow-up period (HR=5.7). However, the differentiation of brain atrophy subtypes during aging and AD requires the categorical classification of subjects within a reference population, which is interesting for epidemiological and pathophysiological studies but not suitable at the individual level in clinical practice (Murray et al., 2011). Although the analysis of hippocampal subfields appears to be a promising biomarker, this technique will require longitudinal rather than cross-sectional volumetric assessments because, as seen in the present study, the normalized hippocampal subfield volumes at baseline were not predictive of Alzheimer’s clinical syndrome whereas the annualized rates of atrophy over 4 years were predictive of the disease. It confirms that the value of longitudinal measures of brain shrinkage usually exceeds that of cross-sectional estimates (Raz et al., 2005) and that such measurements are ultimately more informative.

As mentioned above, the present study has many methodological strengths compared to previous studies in this topic. First, it employed a natural history design that included a large population-based cohort who were monitored with two MRIs (4-year interval) using the same scanner. Second, a very long term prospective follow-up period (14 years) was used, and few participants were lost to follow-up, which allowed for the identification of individuals with “true” healthy aging and the avoidance of a selection bias due to the misclassification of people with presymptomatic neurodegenerative diseases. Third, we performed proper measurements of hippocampal subfields volumes, rather than a “simpler” shape analysis, in conjunction with a strict quality control of the automatic subfields segmentation. Additionally, HIPS, which is an automatic pipeline of hippocampal subfields segmentation was used in this study (Romero et al., 2017). This pipeline is user-friendly and freely available online, which could help to integrate findings across studies.

Regarding the limitations of the study, we acknowledge that volumetric analyses of hippocampal subfields still require protocol harmonization to clearly define subfield boundaries in order to reduce discrepancies between research centers and to obtain a truly standardized and generalizable biomarker (Yushkevich et al., 2015; Olsen et al., 2019). Furthermore, our findings are based on 1.5T MRI. Although it is true that upsampling will never recover completely the underlying high-resolution image, we have previously demonstrated that our post-processing pipeline significantly improve the segmentation results compared to classical interpolation methods such as linear or spline interpolation

(Romero et al., 2017). The main limitation of the present study was the lack of an assessment of amyloid pathologies, which was due to the 1999-2000 inclusion period for the present cohort. Analyses of amyloid pathologies could have further specified the diagnosis of AD and allowed for evaluations of the link between amyloid plaques and the vulnerability of hippocampal subfields. However, the diagnoses of Alzheimer's clinical syndrome (possible or probable AD according to 1984 and 2011 criteria) made in the present study relied on longitudinal assessments and were confirmed by a panel of independent and expert neurologists. Moreover, the present results are congruent with observations from the literature regarding the larger ratio of subjects with incident Alzheimer's disease presenting at least one ApoE4 allele, and the link between CA1-3 atrophy and ApoE4 status specifically in the "incident-AD" subgroup.

Conclusion

In this study, we described the natural history of hippocampal subfield atrophy during healthy aging by pinpointing an increased vulnerability of the dentate gyrus relative to the subiculum and the cornu-ammonis. Although the annualized rate of CA1-3 atrophy was less severe than the other two subfields, it was the only region associated with the risk of developing Alzheimer's clinical syndrome over time, independently of age, gender, educational level and ApoE4 genotype. These findings indicate that aging and AD differentially impact the hippocampal anatomy and that longitudinal MRI measures can contribute to disentangle these two phenomena.

Tables

	Whole cohort (n=327)	Non-AD group (n=269)	Incident-AD group (n=35)	p-value ²
Demographical variables at baseline				
Age, mean (SD)	72.0 (3.8)	71.7 (3.7)	73.7 (3.9)	0.003
Gender, women %	58.2%	57.2%	66.7%	0.28
Education level, high ¹ %	51.8%	51.7%	52.8%	0.90
ApoE (ε4 +/- or +/+), %	20.7%	17.7%	27.8%	0.27
Neuropsychological tests at baseline				
MMSE, median [range]	28 [24-30]	29 [24-30]	28 [24-30]	0.06
FCSRT free recall, mean (SD)	25.1 (5.9)	25.5 (5.7)	22.1 (6.7)	0.002
FCSRT total recall, median [range]	46 [21-48]	46 [21-48]	45 [32-48]	0.08
BVRT, median [range]	12 [6-15]	12 [6-15]	11 [7-15]	0.003
Isaacs set test 15s, mean (SD)	31.4 (5.8)	31.7 (5.7)	29.9 (5.8)	0.07
Isaacs set test 30s, mean (SD)	47.6 (9.1)	48.2 (9.0)	45.1 (9.3)	0.06
Isaacs set test 60s, mean (SD)	70.4 (14.7)	71.5 (14.2)	66.0 (16.5)	0.04
TMT-A, mean (SD)	4.9 (1.5)	5.0 (1.5)	4.2 (1.3)	0.001
TMT-B, mean (SD)	2.3 (1.1)	2.4 (1.1)	2.0 (1.0)	0.05
MRI volumes at baseline				
Hippocampus, mean % ICV (SD)	0.49 (0.04)	0.50 (0.04)	0.49 (0.05)	0.30
CA1-3, mean % ICV (SD)	0.31 (0.03)	0.31 (0.03)	0.30 (0.04)	0.24
CA4-DG, mean % ICV (SD)	0.05 (0.007)	0.05 (0.008)	0.05 (0.009)	0.63
Subiculum, mean % ICV (SD)	0.14 (0.01)	0.14 (0.01)	0.14 (0.02)	0.45

Table 1. Clinical, MRI and neuropsychological features of participants at baseline. BVRT: Benson Visual Retention Test ; FCSRT: Free and Cued Selective Reminding Test ; ICV: IntraCranial Volume ; MMSE: Mini Mental State Examination ; TMT: Trail-Making Test.

1. Education level was considered as high or low according to French baccalaureate (equivalent to A-level).

2. p-values refer to χ^2 test for categorical variables and t-tests for ordinal variables (“non-AD” vs “incident-AD” subgroups)

	ApoE4 +	ApoE4 -	p-value
Whole cohort (n=327 : n=68 ApoE4+ and n=259 ApoE4-)			
Annualized rate of subiculum atrophy, mean (SD)	-1.12 (1.31)	-0.95 (1.10)	0.332
Annualized rate of CA1-3 atrophy, mean (SD)	-0.78 (1.09)	-0.65 (0.85)	0.367
Annualized rate of CA4-DG atrophy, mean (SD)	-1.85 (2.49)	-1.26 (1.92)	0.075
Non-AD group (n=269; : n=48 ApoE4+ and n=221 ApoE4-)			
Annualized rate of subiculum atrophy, mean (SD)	-0.95 (1.28)	-0.93 (1.07)	0.925
Annualized rate of CA1-3 atrophy, mean (SD)	-0.57 (0.99)	-0.60 (0.80)	0.865
Annualized rate of CA4-DG atrophy, mean (SD)	-1.57 (2.36)	-1.19 (1.86)	0.261
Incident-AD group (n=35; n=10 ApoE4+ and n=25 ApoE4-)			
Annualized rate of subiculum atrophy, mean (SD)	-2.12 (1.02)	-1.14 (1.31)	0.028
Annualized rate of CA1-3 atrophy, mean (SD)	-1.98 (0.90)	-1.13 (1.15)	0.030
Annualized rate of CA4-DG atrophy, mean (SD)	-3.46 (2.74)	-1.89 (2.32)	0.131

Table 2: Annualized rate of hippocampal subfields atrophy regarding ApoE4 status in the whole cohort of participants and in both the “non-AD” and “incident-AD” subgroups. ANOVAs p-values not corrected for multiple comparisons. The Bonferroni threshold p-values for 3 comparisons in each group is 0.016.

	Hazard ratio	95% CI
Model 1		
Annualized rate of subiculum atrophy	1.08	0.81-1.47
Annualized rate of CA1-3 atrophy	1.80	1.23-2.63
Annualized rate of CA4-DG atrophy	1.08	0.89-1.32
Model 2		
Age	1.14	1.04-1.26
Gender	1.45	0.69-3.03
Education level	1.18	0.61-2.29
ApoE genotype	1.66	0.79-3.50
Annualized rate of subiculum atrophy	1.04	0.76-1.41
Annualized rate of CA1-3 atrophy	2.00	1.35-2.99
Annualized rate of CA4-DG atrophy	1.07	0.77-1.32

Table 3. Predictive values of annualized rate of hippocampal subfields atrophy alone (model 1) and in combination with age, gender, educational level and ApoE genotype (model 2) on the risk of incident Alzheimer’s clinical syndrome (Cox models).

Figure legends

Figure 1. Datasets. (A) During the follow-up period, neuropsychological assessments (NP) were administered at baseline and after 2, 4, 7, 10, 12 and 14 years. MRI was performed at baseline and 4 years later. (B) Flowchart of the study.

Figure 2. MRI post-processing. (A) To perform the segmentation, the native images (on the left) were first up-sampled with a local adaptive super resolution method (on the right). (B) Examples of hippocampal segmentations in the sagittal and coronal main axis with the HIPS software. The method provides automatic segmentation of hippocampal subfields gathered into 3 labels: Subiculum, CA1-3 and CA4/dentate gyrus (CA4-DG).

Figure 3. Annualized rate of hippocampal subfields atrophy the whole cohort of participants (A) and in participants with future Alzheimer's clinical syndrome and participants who will remain free of AD (B). ** $p < 0.01$ and. *** $p < 0.001$. **** $p < 0.0001$ (Holm-Sidak's multiple comparisons test after one-way ANOVA or Sidak's multiple comparisons test after two-way ANOVA, as appropriate). Cohen's d values measure effect size between two groups.

Acknowledgements and Funding

The 3C Study is conducted under a partnership agreement among the *Institut National de la Santé et de la Recherche Médicale* (INSERM), Bordeaux University, and Sanofi. The *Fondation pour la Recherche Médicale* funded the preparation and initiation of the study. The 3C Study is also supported by *Caisse Nationale Maladie des Travailleurs Salariés*, *Direction Générale de la Santé*, *Mutuelle Générale de l'Éducation Nationale*, *Institut de la Longévité*, *Conseils Régionaux d'Aquitaine et Bourgogne*, *Fondation de France*, and the Ministry of Research-INSERM Programme “*Cohortes et collections de données biologiques*”. The follow-ups have also been funded by ANR 2007LVIE 003, the “*Fondation Plan Alzheimer*” and the Caisse Nationale de Solidarité pour l'Autonomie (CNSA). This work benefited from the support of the project DeepvolBrain of the French National Research Agency (ANR-18-CE45-0013) and by the Spanish DPI2017-87743-R grant from the Ministerio de Economía, Industria y Competitividad of Spain. In addition, this study was achieved within the context of the Laboratory of Excellence TRAIL ANR-10-LABX-57 for the BigDataBrain project. Finally, we thank the Investments for the future Program IdEx Bordeaux (ANR-10- IDEX- 03- 02, HL-MRI Project), Cluster of excellence CPU and the CNRS. VP also received grants from Fondation Bettencourt Schueller (CCA-Inserm-Bettencourt). The sponsors did not participate in any aspect of the design or performance of the study, including data collection, management, analysis, and the interpretation or preparation, review, and approval of the manuscript.

Potential Conflicts of Interest

The authors declare no competing financial interests relative to the present study.

References

- 3C Study Group, 2003. Vascular factors and risk of dementia: design of the Three-City Study and baseline characteristics of the study population. *Neuroepidemiology* 22, 316–325.
- Apostolova, L.G., Green, A.E., Babakchanian, S., Hwang, K.S., Chou, Y.-Y., Toga, A.W., Thompson, P.M., 2012. Hippocampal atrophy and ventricular enlargement in normal aging, mild cognitive impairment (MCI), and Alzheimer Disease. *Alzheimer Dis Assoc Disord* 26, 17–27.
- Auriacombe, S., Helmer, C., Amieva, H., Berr, C., Dubois, B., Dartigues, J.-F., 2010. Validity of the free and cued selective reminding test in predicting dementia: the 3C study. *Neurology* 74, 1760–1767.
- Avants, B.B., Tustison, N.J., Song, G., Cook, P.A., Klein, A., Gee, J.C., 2011. A reproducible evaluation of ANTs similarity metric performance in brain image registration. *NeuroImage* 54, 2033–2044.
- Ball, M.J., Fisman, M., Hachinski, V., Blume, W., Fox, A., Kral, V.A., Kirshen, A.J., Fox, H., Merskey, H., 1985. A new definition of Alzheimer's disease: a hippocampal dementia. *Lancet* 1, 14–16.
- Bobinski, M., de Leon, M.J., Wegiel, J., Desanti, S., Convit, A., Saint Louis, L.A., Rusinek, H., Wisniewski, H.M., 2000. The histological validation of post mortem magnetic resonance imaging-determined hippocampal volume in Alzheimer's disease. *Neuroscience* 95, 721–725.
- Braak, H., Braak, E., 1991. Neuropathological staging of Alzheimer-related changes. *Acta Neuropathol.* 82, 239–259.
- Cao, B., Passos, I.C., Mwangi, B., Amaral-Silva, H., Tannous, J., Wu, M.-J., Zunta-Soares, G.B., Soares, J.C., 2017. Hippocampal subfield volumes in mood disorders. *Mol. Psychiatry* 22, 1352–1358.
- Chételat, G., Fouquet, M., Kalpouzos, G., Denghien, I., De la Sayette, V., Viader, F., Mézenge, F., Landeau, B., Baron, J.C., Eustache, F., Desgranges, B., 2008. Three-dimensional surface mapping of hippocampal atrophy progression from MCI to AD and over normal aging as assessed using voxel-based morphometry. *Neuropsychologia* 46, 1721–1731.
- Coupé, P., Catheline, G., Lanuza, E., Manjón, J.V., Alzheimer's Disease Neuroimaging Initiative, 2017. Towards a unified analysis of brain maturation and aging across the entire lifespan: A MRI analysis. *Hum Brain Mapp* 38, 5501–5518.
- Coupé, P., Manjón, J.V., Chamberland, M., Descoteaux, M., Hiba, B., 2013. Collaborative patch-based super-resolution for diffusion-weighted images. *Neuroimage* 83, 245–261.
- Csernansky, J.G., Wang, L., Joshi, S., Miller, J.P., Gado, M., Kido, D., McKeel, D., Morris, J.C., Miller, M.I., 2000. Early DAT is distinguished from aging by high-dimensional mapping of the hippocampus. *Dementia of the Alzheimer type. Neurology* 55, 1636–1643.
- Daugherty, A.M., Bender, A.R., Raz, N., Ofen, N., 2016. Age differences in hippocampal subfield volumes from childhood to late adulthood. *Hippocampus* 26, 220–228.
- de Flores, R., La Joie, R., Chételat, G., 2015. Structural imaging of hippocampal subfields in healthy aging and Alzheimer's disease. *Neuroscience* 309, 29–50.
- De Flores, R., La Joie, R., Chételat, G., 2015. Structural imaging of hippocampal subfields in healthy aging and Alzheimer's disease. *Neuroscience* 309, 29–50.
- Dillon, S.E., Tsivos, D., Knight, M., McCann, B., Pennington, C., Shiel, A.I., Conway, M.E., Newson, M.A., Kauppinen, R.A., Coulthard, E.J., 2017. The impact of ageing reveals distinct roles for human dentate gyrus and CA3 in pattern separation and object recognition memory. *Sci Rep* 7, 14069.
- Dufouil, C., Richard, F., Fiévet, N., Dartigues, J.F., Ritchie, K., Tzourio, C., Amouyel, P.,

Alpérovitch, A., 2005. APOE genotype, cholesterol level, lipid-lowering treatment, and dementia: the Three-City Study. *Neurology* 64, 1531–1538.

Fouquet, M., Desgranges, B., La Joie, R., Rivière, D., Mangin, J.-F., Landeau, B., Mézence, F., Pélerin, A., de La Sayette, V., Viader, F., Baron, J.-C., Eustache, F., Chételat, G., 2012. Role of hippocampal CA1 atrophy in memory encoding deficits in amnesic Mild Cognitive Impairment. *Neuroimage* 59, 3309–3315.

Frisoni, G.B., Ganzola, R., Canu, E., Rüb, U., Pizzini, F.B., Alessandrini, F., Zoccatelli, G., Beltramello, A., Caltagirone, C., Thompson, P.M., 2008. Mapping local hippocampal changes in Alzheimer's disease and normal ageing with MRI at 3 Tesla. *Brain* 131, 3266–3276.

Hanko, V., Apple, A.C., Alpert, K.I., Warren, K.N., Schneider, J.A., Arfanakis, K., Bennett, D.A., Wang, L., 2019. In vivo hippocampal subfield shape related to TDP-43, amyloid beta, and tau pathologies. *Neurobiology of Aging* 74, 171–181.

Harper, L., Barkhof, F., Scheltens, P., Schott, J.M., Fox, N.C., 2014. An algorithmic approach to structural imaging in dementia. *Journal of Neurology, Neurosurgery & Psychiatry* 85, 692–698.

Ho, N.F., Iglesias, J.E., Sum, M.Y., Kuswanto, C.N., Sitoh, Y.Y., De Souza, J., Hong, Z., Fischl, B., Roffman, J.L., Zhou, J., Sim, K., Holt, D.J., 2017. Progression from selective to general involvement of hippocampal subfields in schizophrenia. *Mol. Psychiatry* 22, 142–152.

Jack, C.R., Bennett, D.A., Blennow, K., Carrillo, M.C., Dunn, B., Haeberlein, S.B., Holtzman, D.M., Jagust, W., Jessen, F., Karlawish, J., Liu, E., Molinuevo, J.L., Montine, T., Phelps, C., Rankin, K.P., Rowe, C.C., Scheltens, P., Siemers, E., Snyder, H.M., Sperling, R., Contributors, 2018. NIA-AA Research Framework: Toward a biological definition of Alzheimer's disease. *Alzheimers Dement* 14, 535–562.

Kerchner, G.A., Berdnik, D., Shen, J.C., Bernstein, J.D., Fenesy, M.C., Deutsch, G.K., Wyss-Coray, T., Rutt, B.K., 2014. APOE ϵ 4 worsens hippocampal CA1 apical neuropil atrophy and episodic memory. *Neurology* 82, 691–697.

Kerchner, G.A., Bernstein, J.D., Fenesy, M.C., Deutsch, G.K., Saranathan, M., Zeineh, M.M., Rutt, B.K., 2013. Shared vulnerability of two synaptically-connected medial temporal lobe areas to age and cognitive decline: a seven tesla magnetic resonance imaging study. *J. Neurosci.* 33, 16666–16672.

Kerchner, G.A., Hess, C.P., Hammond-Rosenbluth, K.E., Xu, D., Rabinovici, G.D., Kelley, D. a. C., Vigneron, D.B., Nelson, S.J., Miller, B.L., 2010. Hippocampal CA1 apical neuropil atrophy in mild Alzheimer disease visualized with 7-T MRI. *Neurology* 75, 1381–1387.

Kulaga-Yoskovitz, J., Bernhardt, B.C., Hong, S.-J., Mansi, T., Liang, K.E., van der Kouwe, A.J.W., Smallwood, J., Bernasconi, A., Bernasconi, N., 2015. Multi-contrast submillimetric 3 Tesla hippocampal subfield segmentation protocol and dataset. *Scientific Data* 2, 150059.

La Joie, R., Fouquet, M., Mézence, F., Landeau, B., Villain, N., Mevel, K., Pélerin, A., Eustache, F., Desgranges, B., Chételat, G., 2010. Differential effect of age on hippocampal subfields assessed using a new high-resolution 3T MR sequence. *Neuroimage* 53, 506–514.

La Joie, R., Perrotin, A., de La Sayette, V., Egret, S., Dœuvre, L., Belliard, S., Eustache, F., Desgranges, B., Chételat, G., 2013. Hippocampal subfield volumetry in mild cognitive impairment, Alzheimer's disease and semantic dementia. *Neuroimage Clin* 3, 155–162.

Lace, G., Savva, G.M., Forster, G., de Silva, R., Brayne, C., Matthews, F.E., Barclay, J.J., Dakin, L., Ince, P.G., Wharton, S.B., MRC-CFAS, 2009. Hippocampal tau pathology is related to neuroanatomical connections: an ageing population-based study. *Brain* 132, 1324–1334.

Li, X., Li, D., Li, Q., Li, Y., Li, K., Li, S., Han, Y., 2016. Hippocampal subfield volumetry in patients with subcortical vascular mild cognitive impairment. *Sci Rep* 6, 20873.

Malykhin, N.V., Huang, Y., Hrybouski, S., Olsen, F., 2017. Differential vulnerability of hippocampal subfields and anteroposterior hippocampal subregions in healthy cognitive aging. *Neurobiol. Aging* 59, 121–134.

Manjón, J.V., Coupé, P., 2016. volBrain: An Online MRI Brain Volumetry System. *Front Neuroinform* 10.

Manjón, J.V., Coupé, P., Martí-Bonmatí, L., Collins, D.L., Robles, M., 2010. Adaptive non-local means denoising of MR images with spatially varying noise levels. *J Magn Reson Imaging* 31, 192–203.

McKhann, G.M., Knopman, D.S., Chertkow, H., Hyman, B.T., Jack, C.R., Kawas, C.H., Klunk, W.E., Koroshetz, W.J., Manly, J.J., Mayeux, R., Mohs, R.C., Morris, J.C., Rossor, M.N., Scheltens, P., Carrillo, M.C., Thies, B., Weintraub, S., Phelps, C.H., 2011. The diagnosis of dementia due to Alzheimer's disease: recommendations from the National Institute on Aging-Alzheimer's Association workgroups on diagnostic guidelines for Alzheimer's disease. *Alzheimers Dement* 7, 263–269.

Mueller, S.G., Schuff, N., Yaffe, K., Madison, C., Miller, B., Weiner, M.W., 2010. Hippocampal atrophy patterns in mild cognitive impairment and Alzheimer's disease. *Hum Brain Mapp* 31, 1339–1347.

Mueller, S.G., Weiner, M.W., 2009. Selective effect of age, Apo e4, and Alzheimer's disease on hippocampal subfields. *Hippocampus* 19, 558–564.

Murray, M.E., Graff-Radford, N.R., Ross, O.A., Petersen, R.C., Duara, R., Dickson, D.W., 2011. Neuropathologically defined subtypes of Alzheimer's disease with distinct clinical characteristics: a retrospective study. *Lancet Neurol* 10, 785–796.

Nyúl, L.G., Udupa, J.K., 1999. On standardizing the MR image intensity scale. *Magnetic Resonance in Medicine* 42, 1072–1081.

Olsen, R.K., Carr, V.A., Daugherty, A.M., La Joie, R., Amaral, R.S.C., Amunts, K., Augustinack, J.C., Bakker, A., Bender, A.R., Berron, D., Boccardi, M., Bocchetta, M., Burggren, A.C., Chakravarty, M.M., Chételat, G., de Flores, R., DeKraaker, J., Ding, S.-L., Geerlings, M.I., Huang, Y., Insausti, R., Johnson, E.G., Kanel, P., Kedo, O., Kennedy, K.M., Keresztes, A., Lee, J.K., Lindenberger, U., Mueller, S.G., Mulligan, E.M., Ofen, N., Palombo, D.J., Pasquini, L., Pluta, J., Raz, N., Rodrigue, K.M., Schlichting, M.L., Lee Shing, Y., Stark, C.E.L., Steve, T.A., Suthana, N.A., Wang, L., Werkle-Bergner, M., Yushkevich, P.A., Yu, Q., Wisse, L.E.M., Hippocampal Subfields Group, 2019. Progress update from the hippocampal subfields group. *Alzheimers Dement (Amst)* 11, 439–449.

Pereira, J.B., Valls-Pedret, C., Ros, E., Palacios, E., Falcón, C., Bargalló, N., Bartrés-Faz, D., Wahlund, L.-O., Westman, E., Junque, C., 2014. Regional vulnerability of hippocampal subfields to aging measured by structural and diffusion MRI. *Hippocampus* 24, 403–414.

Planche, V., Coupé, P., Helmer, C., Le Goff, M., Amieva, H., Tison, F., Dartigues, J.-F., Catheline, G., 2019. Evolution of brain atrophy subtypes during aging predicts long-term cognitive decline and future Alzheimer's clinical syndrome. *Neurobiol. Aging* 79, 22–29.

Planche, V., Koubiyr, I., Romero, J.E., Manjon, J.V., Coupé, P., Deloire, M., Dousset, V., Brochet, B., Ruet, A., Tourdias, T., 2018. Regional hippocampal vulnerability in early multiple sclerosis: Dynamic pathological spreading from dentate gyrus to CA1. *Hum Brain Mapp* 39, 1814–1824.

Postel, C., Viard, A., André, C., Guénolé, F., de Flores, R., Baleyte, J.-M., Gerardin, P., Eustache, F., Dayan, J., Guillery-Girard, B., 2019. Hippocampal subfields alterations in adolescents with post-traumatic stress disorder. *Hum Brain Mapp* 40, 1244–1252.

Raz, N., Daugherty, A.M., Bender, A.R., Dahle, C.L., Land, S., 2015. Volume of the hippocampal subfields in healthy adults: differential associations with age and a pro-inflammatory genetic variant. *Brain Struct Funct* 220, 2663–2674.

Raz, N., Lindenberger, U., Rodrigue, K.M., Kennedy, K.M., Head, D., Williamson, A., Dahle, C., Gerstorf, D., Acker, J.D., 2005. Regional brain changes in aging healthy adults: general trends, individual differences and modifiers. *Cereb. Cortex* 15, 1676–1689.

Romero, J.E., Coupé, P., Manjón, J.V., 2017. HIPS: A new hippocampus subfield segmentation method. *Neuroimage* 163, 286–295.

Sarazin, M., Berr, C., De Rotrou, J., Fabrigoule, C., Pasquier, F., Legrain, S., Michel, B., Puel, M., Volteau, M., Touchon, J., Verny, M., Dubois, B., 2007. Amnesic syndrome of the medial temporal type identifies prodromal AD: a longitudinal study. *Neurology* 69, 1859–1867.

Sarazin, M., Chauviré, V., Gerardin, E., Colliot, O., Kinkingnehun, S., de Souza, L.C., Hugonot-Diener, L., Garnero, L., Lehericy, S., Chupin, M., Dubois, B., 2010. The amnesic syndrome of hippocampal type in Alzheimer's disease: an MRI study. *J. Alzheimers Dis.* 22, 285–294.

Scheltens, P., Leys, D., Barkhof, F., Huglo, D., Weinstein, H.C., Vermersch, P., Kuiper, M., Steinling, M., Wolters, E.C., Valk, J., 1992. Atrophy of medial temporal lobes on MRI in "probable" Alzheimer's disease and normal ageing: diagnostic value and neuropsychological correlates. *J. Neurol. Neurosurg. Psychiatry* 55, 967–972.

Small, S.A., Schobel, S.A., Buxton, R.B., Witter, M.P., Barnes, C.A., 2011. A pathophysiological framework of hippocampal dysfunction in ageing and disease. *Nat. Rev. Neurosci.* 12, 585–601.

Sone, D., Sato, N., Maikusa, N., Ota, M., Sumida, K., Yokoyama, K., Kimura, Y., Imabayashi, E., Watanabe, Y., Watanabe, M., Okazaki, M., Onuma, T., Matsuda, H., 2016. Automated subfield volumetric analysis of hippocampus in temporal lobe epilepsy using high-resolution T2-weighted MR imaging. *Neuroimage Clin* 12, 57–64.

Sorrells, S.F., Paredes, M.F., Cebrian-Silla, A., Sandoval, K., Qi, D., Kelley, K.W., James, D., Mayer, S., Chang, J., Auguste, K.I., Chang, E.F., Gutierrez, A.J., Kriegstein, A.R., Mathern, G.W., Oldham, M.C., Huang, E.J., Garcia-Verdugo, J.M., Yang, Z., Alvarez-Buylla, A., 2018. Human hippocampal neurogenesis drops sharply in children to undetectable levels in adults. *Nature* 555, 377–381.

Tang, X., Holland, D., Dale, A.M., Younes, L., Miller, M.I., Alzheimer's Disease Neuroimaging Initiative, 2014. Shape abnormalities of subcortical and ventricular structures in mild cognitive impairment and Alzheimer's disease: detecting, quantifying, and predicting. *Hum Brain Mapp* 35, 3701–3725.

Tustison, N.J., Avants, B.B., Cook, P.A., Gee, J.C., 2010. N4ITK: Improved N3 bias correction with robust B-spline approximation, in: *IEEE ISBI 2010*. <https://doi.org/10.1109/ISBI.2010.5490078>

West, M.J., Coleman, P.D., Flood, D.G., Troncoso, J.C., 1994. Differences in the pattern of hippocampal neuronal loss in normal ageing and Alzheimer's disease. *Lancet* 344, 769–772.

Yushkevich, P.A., Amaral, R.S.C., Augustinack, J.C., Bender, A.R., Bernstein, J.D., Boccardi, M., Bocchetta, M., Burggren, A.C., Carr, V.A., Chakravarty, M.M., Chetelat, G., Daugherty, A.M., Davachi, L., Ding, S.-L., Ekstrom, A., Geerlings, M.I., Hassan, A., Huang, Y., Iglesias, E., La Joie, R., Kerchner, G.A., LaRocque, K.F., Libby, L.A., Malykhin, N., Mueller, S.G., Olsen, R.K., Palombo, D.J., Parekh, M.B., Pluta, J.B., Preston, A.R., Pruessner, J.C., Ranganath, C., Raz, N., Schlichting, M.L., Schoemaker, D., Singh, S., Stark, C.E.L., Suthana, N., Tompary, A., Turowski, M.M., Van Leemput, K., Wagner, A.D., Wang, L., Winterburn, J.L., Wisse, L.E.M., Yassa, M.A., Zeineh, M.M., 2015. Quantitative Comparison of 21 Protocols for Labeling Hippocampal Subfields and Parahippocampal Subregions in In Vivo MRI: Towards a Harmonized Segmentation Protocol. *Neuroimage* 111, 526–541.

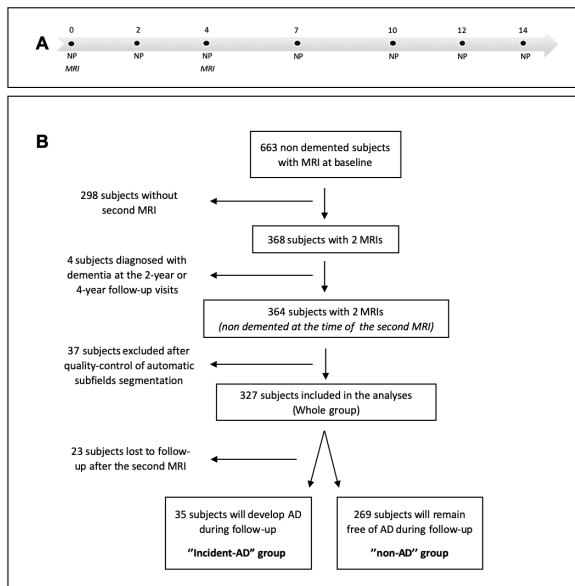


Figure 1

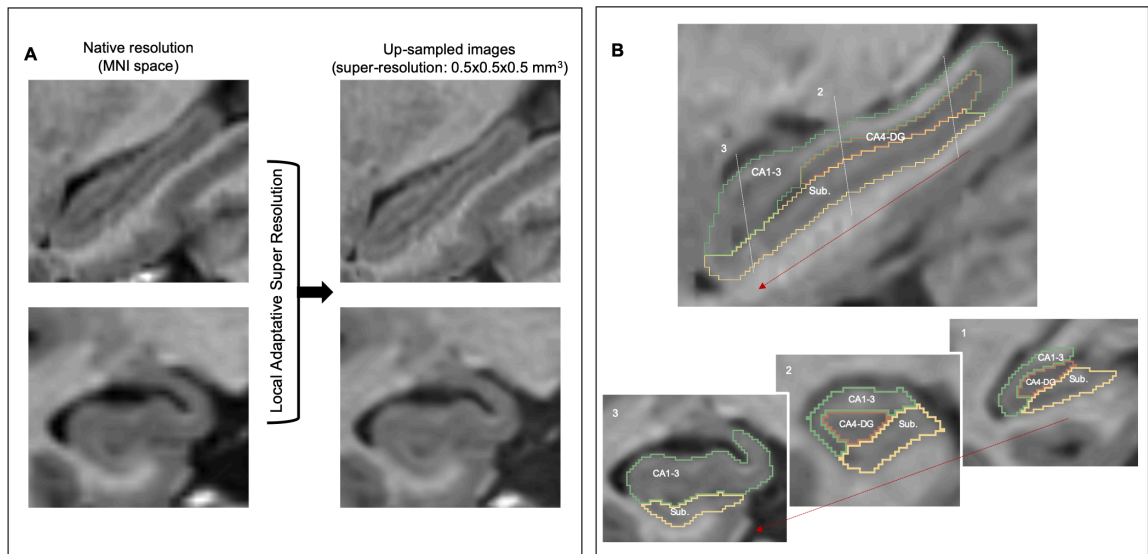


Figure 2

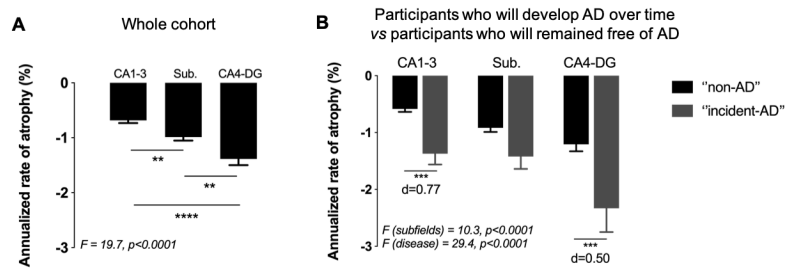


Figure 3